AURA 2008 Science Team

Carbon Monoxide in the High Latitude Polar Stratosphere and Mesosphere

K. Minschwaner[1], G.L. Manney[2,1], N. J. Livesey[2], H. C. Pumphrey[3], H. M. Pickett[2], P. F. Bernath[4,5], and C. D. Boone[4]

1. *Department of Physics, New Mexico Tech*
2. *Jet Propulsion Laboratory, California Institute of Technology*
3. *School of Geosciences, The University of Edinburgh*
4. *Department of Chemistry, University of Waterloo*
5. *Department of Chemistry, University of York*

Abstract: The photochemisty and transport of carbon monoxide (CO) in the high latitude stratosphere and mesosphere can be evaluated using observations from the Aura Microwave Limb Sounder (MLS) and the Atmospheric Chemistry Experiment-Fourier Transform Spectrometer (ACE-FTS). Simultaneous measurements of the reactive species involved in the photochemistry of CO are used to constrain rates for chemical production and loss. This work is focused particularly on high latitude regions during the winter/spring seasons in order to interpret the observed evolution of CO and its relation to the effects of downward transport from the mesosphere into the stratospheric polar vortex.

Copyright 2008 California Institute of Technology.
Government Sponsorship Acknowledged.

CO Photochemistry

In the stratosphere and mesosphere, the production and loss of carbon monoxide involves just five reactions:

CO loss: $CO + OH \rightarrow CO_2 + H$

CO production:
$CH_4 + OH \rightarrow CO + products$
$CH_4 + O(^1D) \rightarrow CO + products$
$CH_4 + Cl \rightarrow CO + products$
$CO_2 + h\nu \rightarrow CO + O$

Blue species above are measured directly by the Microwave Limb Sounder (MLS) on Aura: CO and OH

Red species above can be inferred or calculated using constraints from MLS: CH_4 $O(^1D)$ and Cl

In addition, MLS-measured temperatures are used for calculating chemical reaction rates.

CO Vertical Transport

At high latitudes in winter and early spring, the dominant vertical motion is downward in connection with very large rates for radiative cooling (as indicated below).

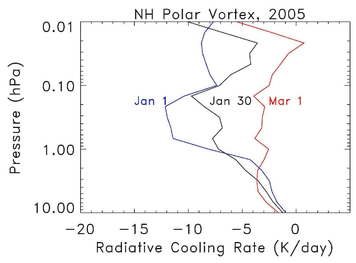

This figure shows radiative cooling rates calculated using MLS ozone and zonal mean temperatures at 70°N for three days during NH winter. Adopted from *Manney et al JGR, 2007JD009097*.

In general, the mixing ratio of CO increases with height from the stratosphere to mesosphere, as seen below in zonal averages from MLS measurements for the NH spring.

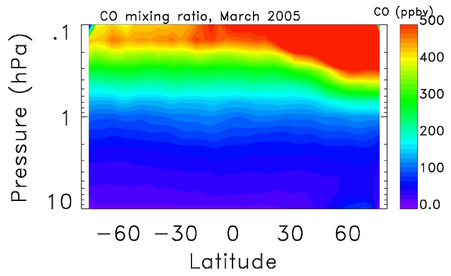

The combination of large vertical gradients and downward motion leads to increasing CO within the polar stratosphere during winter, as seen above.

The descent of CO-rich air from the mesosphere into the stratosphere is clearly seen in the winter/spring evolution of vortex-average CO shown below. One goal of this work is to understand the interplay between transport and photochemistry in controlling both the distribution and time evolution of CO in the high latitude stratosphere.

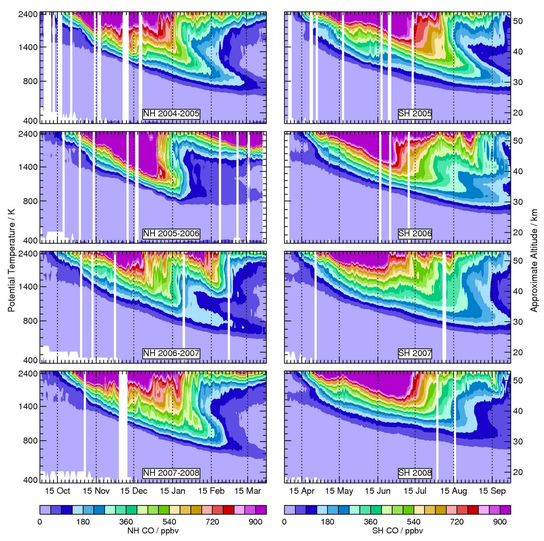

Vortex average CO mixing ratio within an sPV contour of 1.4 x 10^{-4} s^{-1} (e.g. *Manney et al., JAS, 1994*), with sPV from GEOS4/5 and MLS v2.2 CO.

Hydroxyl (OH):

OH varies significantly with solar zenith angle, and diurnal effects are thus present in the MLS OH data. As the lifetime of CO is expected to be much longer than one day throughout the stratosphere and mesosphere, 24-hour average rates must be computed.

We developed an **observationally based diurnal estimation of OH** using MLS measurements. Equation (1) below is based on the expectation that OH responds primarily to the actinic flux responsible for ozone photolysis (e.g. *Canty and Minschwaner, JGR, 2002JD002278*).

$$OH(t) = OH_o \exp[- 0.5 \tau_{O3} \sec\{\theta(t-\varphi)\}] \qquad \text{(eq 1)}$$

where t = time
τ_{O3} = ozone vertical optical depth
θ = solar zenith angle at phase-lagged time t-φ
φ = time phase lag of 0.5 hour (*Li et al, GRL 2005*)
OH_o=peak hydroxyl concentration (for θ=0)

At each MLS observation point, τ_{O3} is obtained from the measured ozone overburden and a weighted mean cross section σ=1.2x10^{-18} cm^2. OH_o is a simple boundary condition that can be determined from a single MLS OH measurement.

The figures below show results from at three latitudes, and a comparison of the derived diurnal range measured by the FIRS2 in situ balloon instrument.

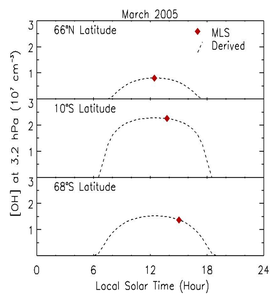

Diurnal concentrations of OH at the 3.2-hPa pressure level based on equation (1) and MLS measurements of OH and O_3 overburden (dashed curves). Also shown are the individual MLS OH measurements (red symbols).

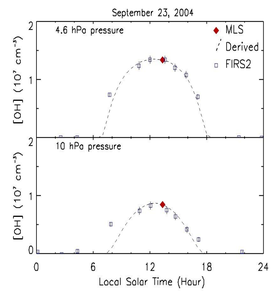

Diurnal concentrations of OH at 4.6 (top) and 10 hPa (bottom) pressure levels based on eq (1) (dashed curves) and corresponding MLS measurements (red triangles) at the lat/lon closest to a Sept 2004 balloon flight. Also shown are balloon-borne measurements of OH from FIRS2 (open squares). FIRS2 data provided by K. Jucks.

CO loss rate due to reaction with OH: The diurnally-averaged, zonal mean OH concentration is shown below for March 2005. Also shown are CO loss rates based on MLS CO and OH. The temperature dependent reaction rate is from JPL evaluation #15 (Sander et al, 2006). Note that the peak loss of about 5x10^3 cm^{-3} s^{-1} occurs near 2 hPa at low/mid latitudes, which arises primarily from the distribution of OH.

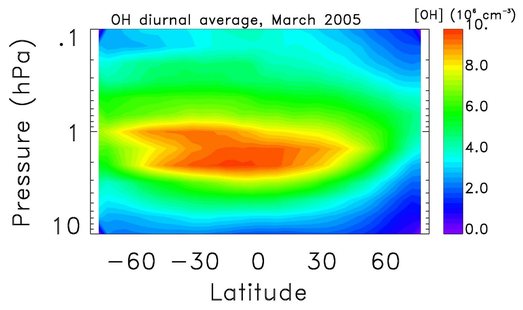

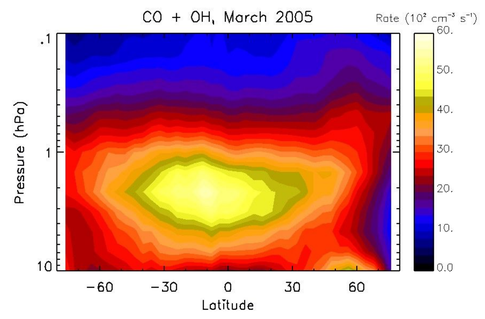

Methane (CH_4):

There are no simultaneous measurements of CH_4 with MLS OH; however there is a correspondance between CH_4 and H_2O in the stratosphere and mesosphere as seen in a correlation density plot of data from the Atmospheric Chemistry Experiment – Fourier Transform Spectrometer (ACE-FTS).

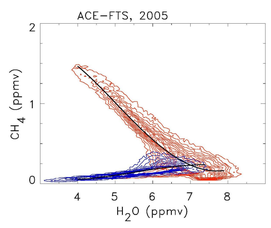

The form of the H_2O - CH_4 relationship is set primarily by oxidation of CH_4 to H_2O (red contours). When there is loss of CH_4 and H_2O by photodissociation, then the relationship transitions to a different regime (blue contours). The threshold for this transition is accurately quantified using a CO level of 0.25 ppb. We use a 2-part functional form:
(i) Where CO<0.25ppm, H_2O amounts are determined primarily by stratospheric entry plus CH_4 oxidation (upper black curve)
(ii) Where CO>0.25ppm, loss of both H_2O and CH_4 is (or has been) significant (lower black curve). This state occurs frequently above 55 km or within the polar vortices.

CO production from CH_4+OH: The figures below show the CH_4 distribution based on MLS H_2O and CO, and corresponding CO production rates from the reaction CH_4+OH. Compared to CO loss, this production rate is roughly a factor of 4 smaller in magnitude and is constrained to lower altitudes and more equatorial latitudes. The differences are primarily the result of the distribution of CH_4.

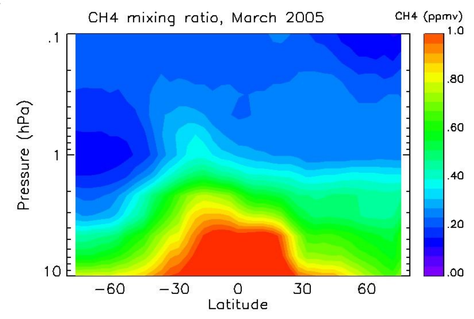

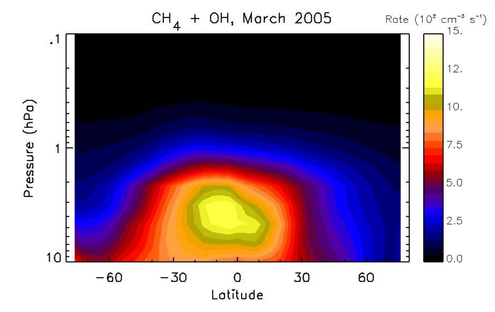

CO production from CH_4+Cl: CH_4 is from MLS H_2O and CO as above, and Cl is determined using MLS HCl and OH: Cl ~ (k_1[HCl][OH])/(k_2[CH_4]), where k_1 and k_2 are the reaction rates for OH+HCl, and CH_4+Cl, respectively.

The figures below show the derived Cl mixing ration for March 2005, and the CO production rate from the reaction CH_4+Cl.

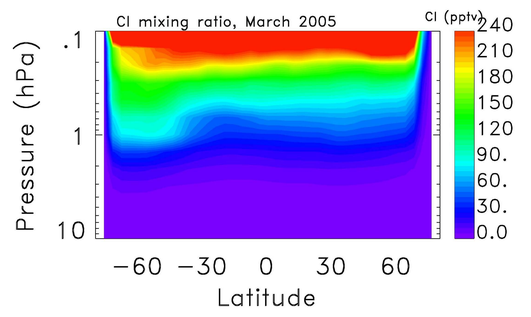

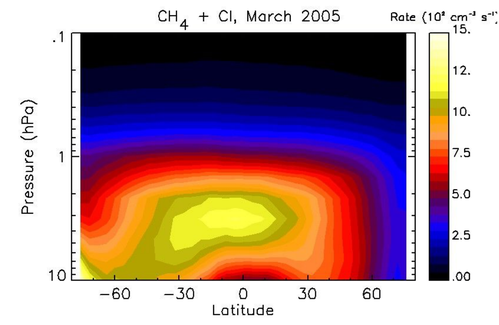

CO production from CH_4+$O(^1D)$: $O(^1D)$ is calculated using steady-state photochemistry and MLS-measured O_3 and O_3 overburden for the photodissociation frequency of ozone, J_{O3}. Production rates (below) are roughly the same magnitude as the other two rates but the distribution is more sharply peaked in latitude and occurs at a lower altitude, primarily as a result of the distribution of ozone.

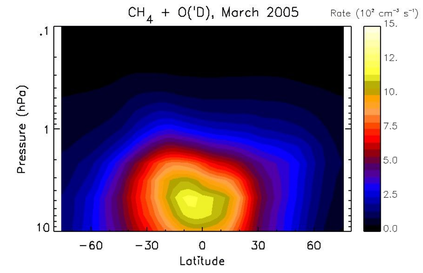

CO production from CO_2+hv: The figure below shows the calculated CO production rate from CO_2 photolysis. Rates at altitudes above the 1 hPa pressure level are much larger than for the CH_4 production reactions, and in fact this photolysis is responsible for increasing CO amounts in the mesosphere.

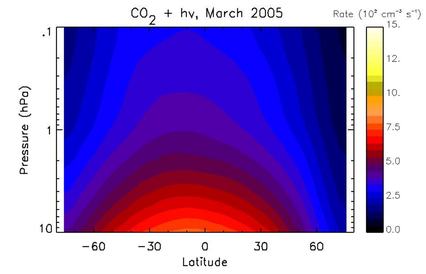

CO lifetimes:

The figures below compare net loss and production lifetimes for CO. Loss generally dominates over production between 10 and 0.1 hPa, with lifetimes of ~ 10-20 days in the upper stratosphere. Photochemical times are longer in the springtime polar regions, but can approach 20 days near 1 hPa and ~ 65° latitude. These times are sufficiently short that photochemistry can play a role in the evolution of CO in the polar vortex.

Zonal mean photochemical lifetimes for CO using the MLS-based production and loss rates shown previosuly for March, 2005. Top panel shows the 1/e destruction timescale; bottom panel is the x2 production timescale.

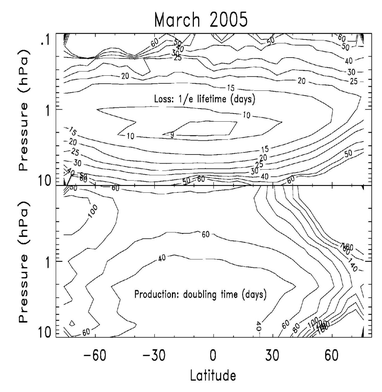

Zonal mean photochemical lifetimes for CO using the MLS-based production and loss rates for September, 2005. Top panel shows the 1/e destruction timescale; bottom panel is the x2 production timescale.

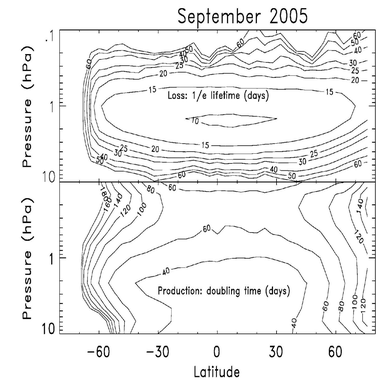
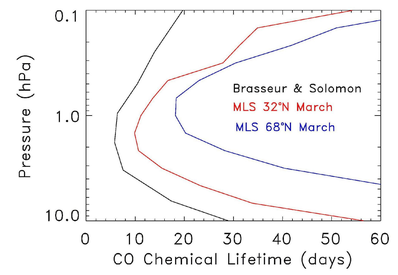
Comparison of CO lifetimes: Shown below are results from (i) model global mean from Brasseur and Solomon, (ii) MLS-based at mid latitudes, (iii) MLS-based at high latitudes. The MLS-based lifetimes are generally longer than those found in previous model calculations.